Rapid Tracking of Small Displacements Using Ultrasound

Gianmarco F. Pinton, Jeremy J. Dahl, and Gregg E. Trahey
Department of Biomedical Engineering
Duke University, Durham, NC 27708

***Abstract*— Time delay estimators, such as normalized cross correlation and phase shift estimation, form the computational basis for elastography, blood flow measurements and Acoustic Radiation Force Impulse (ARFI) imaging. This paper examines the performance of these algorithms for small displacements (less than half the ultrasound pulse wavelength). The effects of noise, bandwidth, downsampling, interpolation, and quadrature demodulation on the accuracy of the time delay estimates are measured in terms of bias and jitter.**

I. Introduction

Several clinical applications depend on the accurate estimation of displacement between successively acquired ultrasound frames. Acoustic Radiation Force Impulse (ARFI) imaging is a radiation force based imaging method that provides information about the local mechanical properties of tissue[1]. ARFI imaging uses short duration acoustic radiation forces to generate localized displacements in tissue, and these displacements are tracked using ultrasonic correlation based methods.

Elastography, Doppler flow, or Doppler tissue measurements use techniques similar to ARFI imaging to calculate motion. Displacements in ARFI imaging are normally orders of magnitude smaller than other modalities. ARFI generates displacements on the order of a tenth to a hundredth of the ultrasound wavelength (λ), elastography measures displacements of 10λ, Doppler flow is usually greater than $\lambda/10$, and Doppler tissue measurements are usually greater than $\lambda/20$.

This paper examines displacements in the ARFI imaging range using three time delay estimators: normalized cross correlation, Kasai's algorithm[2], and Loupas' algorithm[3]. We compare the performance of these algorithms for general RF parameters, such as bandwidth and noise, and parameters specific to ultrasound scanners, such as downsampling of baseband RF.

II. Methods

A. Phase Shift Estimation

Kasai *et al.* phase shift estimation algorithm[2] uses I/Q data to determine the displacement between a reference and a displaced signal by measuring the average phase-shift with respect to the central frequency (see eqn. 1, next page).

The variable $\bar{u}$ is the average displacement estimate for a given axial range, M, and an ensemble length of N. The I/Q components of the RF signal are calculated using trigonometric quadrature demodulation.

Loupas *et al.* two dimensional autocorrelator[3] is show as eqn. 2 (next page). The variable f_{dem} is ratio of the RF sampling rate to the sampling frequency of the signal (hence, $f_{dem} = 5.0\text{MHz}/40\text{MHz}$). Kasai's phase shift estimator assumes a constant mean frequency of the RF equal to the center frequency of the transducer. Loupas' algorithm evaluates the mean Doppler frequency and the mean RF frequency along each axial extent.

B. Normalized Cross Correlation

Normalized cross correlation has the best performance by most measures relevant to time delay estimation in ultrasonic signals[4]. The correlation function $c(j)$, between the reference, f_r, and shifted, f_s, signals is normalized by their standard deviation:

$$c(j) = \frac{\sum_{i=-M/2}^{M/2} \left[f_r(i) - \bar{f}_r\right]\left[f_s(i+j) - \bar{f}_s(j)\right]}{\sqrt{\sum_{i=-M/2}^{M/2} \left[f_r(i) - \bar{f}_r\right]^2 \sum_{i=-M/2}^{M/2} \left[f_s(i+j) - \bar{f}_s(j)\right]^2}} \tag{3}$$

where $\bar{f}_r$ is the mean of the reference value over a window of size M and $\bar{f}_s(j)$ is the mean over a window shifted by j samples. The maximum of the normalized cross correlation function indicates the point where two signals are most similar to each other, and can thus be used to determine the displacement between the reference and tracking lines in ARFI.

C. Bias and Jitter

Bias is the mean of the displacement error and jitter represents the error for the bias, i.e. jitter is measured as the standard deviation of the displacement error. Signal decorrelation, finite window lengths, and noise cause slight shifts in the peak of a correlation function[5].

D. RF data simulation

RF data was constructed to simulate line scatterers moving axially toward the transducer. A Gaussian enveloped RF pulse was convolved with white noise in order simulate the echo received when an ultrasound pulse is reflected from random scatterers. Where stated, Gaussian white noise was added to the reference and displaced signals. Unless otherwise specified, the RF lines used in the calculations and plots shown below have a sampling frequency of 40MHz, a fractional bandwidth of 0.7, a center frequency of 5 MHz, 2000 samples,

$$\bar{u} = \frac{c}{4\pi f_c} \arctan \left(\frac{\sum_{n=0}^{N-2} \left[\sum_{m=0}^{M-1} Q(m,n) \sum_{m=0}^{M-1} I(m,n+1) - \sum_{m=0}^{M-1} I(m,n) \sum_{m=0}^{M-1} Q(m,n+1) \right]}{\sum_{n=0}^{N-2} \left[\sum_{m=0}^{M-1} I(m,n) \sum_{m=0}^{M-1} I(m,n+1) + \sum_{m=0}^{M-1} Q(m,n) \sum_{m=0}^{M-1} Q(m,n+1) \right]} \right) \tag{1}$$

$$\bar{u} = \frac{c}{4\pi f_c} \frac{\arctan \left(\frac{\sum_{m=0}^{M-1} \sum_{n=0}^{N-2} [Q(m,n)I(m,n+1) - I(m,n)Q(m,n+1)]}{\sum_{m=0}^{M-1} \sum_{n=0}^{N-2} [I(m,n)I(m,n+1) + Q(m,n)Q(m,n+1)]} \right)}{1 + \arctan \left(\frac{\sum_{m=0}^{M-2} \sum_{n=0}^{N-1} [Q(m,n)I(m+1,n) - I(m,n)Q(m+1,n)]}{\sum_{m=0}^{M-2} \sum_{n=0}^{N-1} [I(m,n)I(m+1,n) + Q(m,n)Q(m+1,n)]} \right) / (2\pi f_{dem})} \tag{2}$$

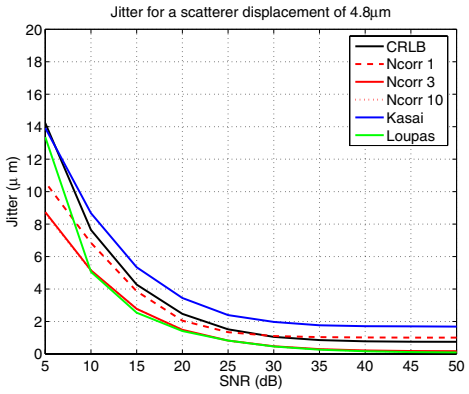

Fig. 1. Jitter error comparison as a function of noise

100 independent realizations, and the algorithms have an axial extent of 1.5λ.

III. Results

A. RF Interpolation

Figure 1 plots the jitter between the reference and displaced signal for varying SNR using different rf interpolation factors for the first interpolation stage. For normalized cross correlation there is little benefit in interpolating the RF data beyond a factor of three. Loupas' algorithm is comparable to normalized cross correlation except at small SNR. Kasai's algorithm has significantly more jitter than other methods. An interpolation factor of three is used for the rest of this paper.

B. Displacement

Figure 2 shows the jitter (top) and bias (bottom) for an SNR of 30dB as the scatterer displacement is varied. Normalized cross correlation has the smallest jitter across the displacement range, followed by Loupas' and then Kasai's algorithm. Loupas' algorithm develops an increasing bias toward overestimation as the displacement increases. Kasai's algorithm follows an opposite and more significant trend toward underestimation of displacement.

C. Step Displacement

Algorithms that use a smaller axial extent are able to discern the step displacement with a steeper slope. Figure 3 plots the

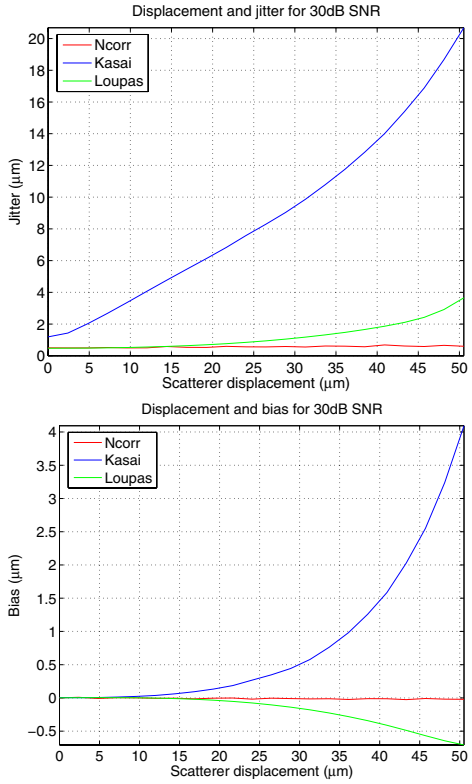

Fig. 2. Jitter (top) and bias (bottom) for varying scatterer displacement.

displacement for various axial extents (expressed as fractions of the pulse wavelength). Normalized cross correlation and Loupas' algorithm have comparable performance in resolving the step displacements for an axial extent of 1.5λ and 3λ but the performance of Loupas' algorithm is significantly degraded for 0.5λ. Kasai's algorithm exhibits the largest amount of jitter.

D. Bandwidth

Figure 4 shows how the signal bandwidth affects phase shift estimators to a larger degree than normalized cross correlation. Loupas' algorithm performs well except for a broadband signal. Kasai's algorithm exhibits a more regular increase in jitter with bandwidth.

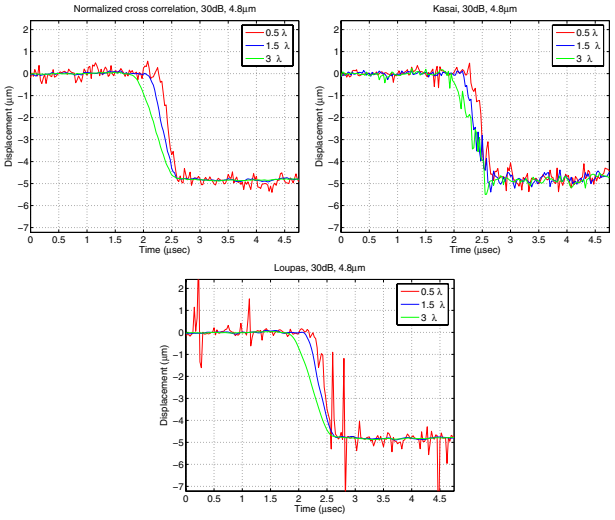

Fig. 3. Comparison of step displacement tracking between the time delay algorithms for varying kernel lengths.

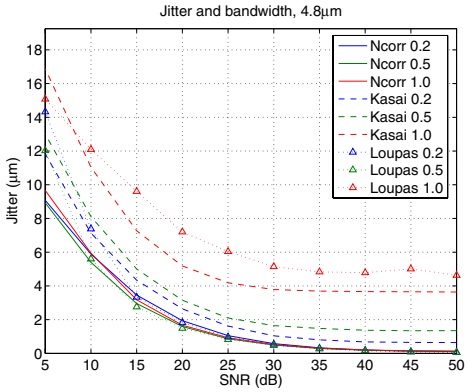

Fig. 4. Jitter comparison between the time delay algorithms with different different fractional bandwidths.

E. Down-sampling

Figure 5 shows effects of downsampling on the jitter (top) and bias (bottom) for the time delay algorithms. A demodulated RF signal normally has a sampling frequency that is much higher than the Nyquist frequency so the data can be down-sampled without aliasing. The jitter for Loupas' algorithm on the down-sampled I/Q increases dramatically with down-sampling factor until it reaches an axial extent of one sample and matches Kasai's algorithm. This suggests that given an insufficient number of samples the frequency correction of Loupas' algorithm becomes inaccurate. However by allowing Loupas' algorithm to operate on more elements by up-sampling the down-sampled I/Q a close match with normalized cross correlation can be achieved. For a small displacement of $4.8\mu m$, normalized cross correlation on the remodulated RF data often has a higher bias toward underestimation than the phase shift algorithms.

F. Ex Vivo Liver Ablation

ARFI images of an *ex-vivo* liver ablation with the displacement shown in microns. On the top rows are images

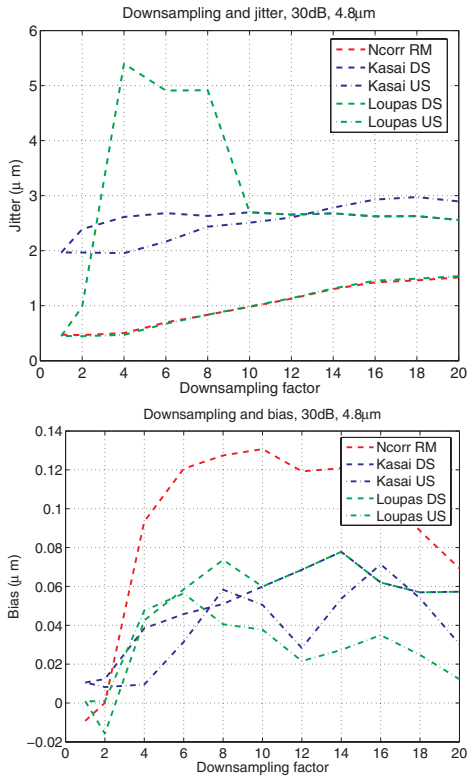

Fig. 5. The effects of down-sampling on jitter (top) and bias (bottom) for normalized cross correlation on the remodulated signal (Ncorr RM), Kasai's phase shift estimation algorithm on the down-sampled (Kasai DS), and up-sampled I/Q (Kasai US), and Loupas' phase shift estimation algorithm on the down-sampled (Loupas DS), and up-sampled I/Q (Loupas US).

generated from the original data. In the middle row, the phase shift estimators are applied to the down-sampled I/Q data. On the bottom row, the images are generated with the down-sampled, then up-sampled data (down-sampling factor of 8). The lesion can be observed as the stiffer (less displaced) region at the center right of each image. Figure 7 shows a degassed bovine liver after 12 minutes of preprogrammed ablation. Images generated by normalized cross correlation or Loupas' algorithm appear less noisy, have better edge definition, and a higher CNR. Loupas' algorithm appears to be more noisy than normalized cross correlation in the bottom portion of the images where the SNR is low. However the difference between the two is almost indistinguishable on the up-sampled images. The phase shift estimators applied to the down-sampled I/Q generate noisy images with poor edge definition.

G. Real-time Implementation

A Siemens Antares scanner ports the raw 40 MHz RF data to an adjacent Beowolf cluster via a 100 Mbit Ethernet link. The cluster consists of 8 Dell Optiplex SX270 compute nodes. Each node has a 3.0 GHz Pentium 4 processor and 1 GB of RAM. The nodes are connected via gigabit ethernet to a Dell PowerConnect 5224 switch. All the systems run CentOS 3.3, a free version of Red Hat Enterprise Linux 3. Parallel processing and internode communication is handled with version 6.5.9 of the LAM/MPI toolkit. The algorithms were implemented with

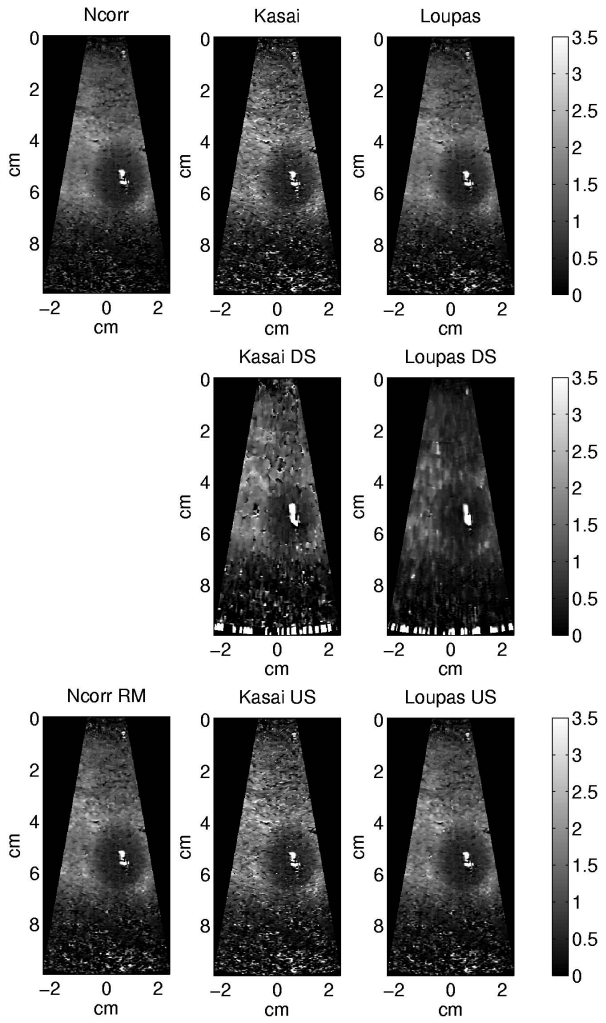

Fig. 6. ARFI images of an *ex-vivo* liver ablation with the displacement shown in microns. On the top rows are images generated from the original data. In the middle row, the phase shift estimators are applied to the down-sampled I/Q data. On the bottom row, the images are generated with the down-sampled, then up-sampled data (down-sampling factor of 8). The lesion can be observed as the stiffer (less displaced) region at the center right of each image.

a combination of Fortran77 and C.

H. Computational Time

To reduce the computational load, the algorithms are calculated using a sliding window scheme for the numerators and the denominators. Loupas' and Kasai's algorithms are less computationally intensive than normalized cross correlation but have a similar slope or order. There is little difference in the computation times for different window sizes when a small overlap is used. However, with increasing overlap it becomes more costly to use larger windows. There is a negligible effect of window size on the phase shift estimators.

IV. Conclusion

We have shown the performance differences between normalized cross correlation, Loupas' and Kasai's algorithms in terms of displacement errors in the form of jitter and bias and parameter selection such as kernel size, signal bandwidth,

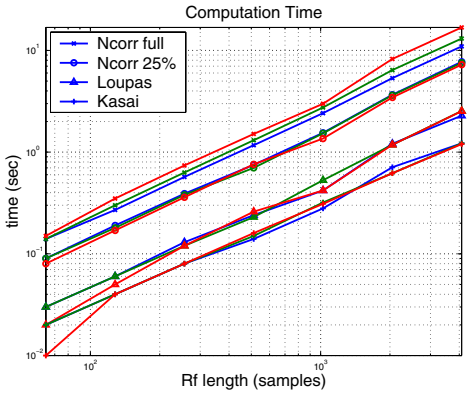

Fig. 7. Computational time to determine the scatterer displacement as a function of the number of RF samples. The top three curves (crosses) show normalized cross correlation with full overlap and window sizes of 0.75λ (solid), 1.5λ (dashed), 3λ (dash-dotted), indicating larger windows require longer calculation times. Beneath these three curvesare the times for normalized cross correlation with 25% overlap (circles), Loupas' (triangles), and Kasai's (plus signs) algorithms.

TABLE I
TYPICAL ARFI COMPUTATIONAL TIMES

	Single line	Serial image	Parallel image
Kasai	0.21 ms	51 ms	14 ms
Loupas	0.39 ms	58 ms	17 ms
Correlation	2.25 ms	204 ms	40 ms

and interpolation factors. Kasai's algorithm generally has the worst performance and the fastest computation time. Loupas' algorithm performs almost as well as normalized cross correlation except for cases where the axial extent is small and the SNR is low or when the bandwidth is large. We have shown how to accurately reconstruct displacement calculations using down-sampled I/Q data. Finally, the optimal algorithmic parameters were used in a parallel program to implement a real-time ARFI imaging system on a computer cluster and an associated ultrasound scanner.

V. Acknowledgments

The authors thank the Ultrasound Division at Siemens Medical Solutions USA, Inc. for their in kind and technical support. This work was supported by the NIH grants R01-HL07548501, 1R01CA114093-01, and R01-EB002132.

References

[1] K. Nightingale, M. Soo, R. Nightingale, and G. Trahey, "Acoustic radiation force impulse imaging: In vivo demonstration of clinical feasibility," *Ultrasound Med. Biol.*, vol. 28, no. 2, pp. 227–235, 2002.

[2] C. Kasai, K. Namekawa, A. Koyano, and R. Omoto, "Real-time two-dimensional blood flow imaging using autocorrelation technique," *IEEE Trans. Son. Ultrason.*, vol. 32, pp. 458–463, 1985.

[3] T. Loupas, R. Peterson, and R. Gill, "Experimental evaluation of velocity and power estimation for ultrasound blood flow imaging, by means of a two-dimensional autocorrelation approach," *IEEE Trans. Ultrason., Ferroelect., Freq. Contr.*, vol. 42, pp. 689–699, 1995.

[4] F. Viola and W. F. Walker, "Comparison of time delay estimators in medical ultrasound," in *Proc. 2001 IEEE UFFC*, 2001.

[5] W. F. Walker and G. E. Trahey, "A fundamental limit on delay estimation using partially correlated speckle signals," *IEEE Trans. Ultrason., Ferroelect., Freq. Contr.*, vol. 42, no. 2, pp. 301–308, March 1995.